Photoluminescence spectroscopy of defects in ZnO nano/microwires

Sun Xiang-Bing(孙香冰)[a], Feng Lin(冯 林)[b]†, and Jiao Xian-Wei(焦现炜)[a]

[a]72465 *Unit of the PLA, Jinan* 250022, *China*

[b]*School of Physics, Shandong University, Jinan* 250100, *China*

(Received 29 August 2010; revised manuscript received 8 October 2010)

Photoluminescence spectroscopy is used to study defects found in single ZnO nano/microwires at 90 K. The defect, acting as binding site for bound exciton (BX) transition, is represented by $B_{\rm F}$, the fractional intensity of the BX peak in the whole near-band edge ultraviolet (UV) luminescence. The concentration of defects as origins of the visible emissions is proportional to the intensity fraction $D_{\rm F}$, i.e., the intensity fraction of visible emissions in the sum total of all UV and visible luminescences. By comparing $B_{\rm F}$ and $D_{\rm F}$, it is concluded that the two defects are not correlated to each other. The former kind of defect is considered to be related to the blueshift of the near-band edge peak as the radius of the nano/microwires decreases at room temperature.

Keywords: ZnO, photoluminescence, defect

PACS: 78.55.–m, 78.55.Et, 42.62.Fi, 61.46.Km **DOI:** 10.1088/1674-1056/20/6/067804

1. Introduction

ZnO is of great interest due to its potential applications in optoelectronic devices such as light emitting diodes.[1] Generally, the intrinsic luminescence in the photoluminescence (PL) spectrum of ZnO is the near-band-edge (NBE) ultraviolet (UV) emission due to exciton-related recombinations.[2] The appearance of green and/or yellow bands is a fingerprint of the presence of the ZnO defects. We denote the defects responsible for these visible so-called defect-related emissions (DEs) by $\rm DFT_{Vis}$. Moreover, defects are also relevant to NBE luminescence. At low temperature, fine peaks of UV emission can be discriminated and some of them are from bound exciton (BX) transitions. The binding sites for BXs are kinds of defects $\rm DFT_{BX}$. There has been no consensus of opinion on the nature of $\rm DFT_{Vis}$ and $\rm DFT_{BX}$[3,4] and their possible relations. Cui[5] assumed that the NBE peak wavelength could be determined by $\rm DFT_{Vis}$ and reported its red shift at room temperature (RT) with a larger relative intensity of DE, in contrast to the blue shift by some other groups.[6,7] Therefore, it is important to provide more concrete information for determining whether the two categories of defects, $\rm DFT_{Vis}$ and $\rm DFT_{BX}$, are correlated to each other, and whether $\rm DFT_{Vis}$ affects the UV peak position.

In the present work, PL investigations are carried out on single ZnO nano/microwires at 90 K. The fractional intensity of the BX peak in the overall NBE UV luminescence, $B_{\rm F}$, decreases as the sample size increases. However, there is no monotonic relationship between the size and $D_{\rm F}$, the intensity fraction of DE in all UV and visible emissions. Thus, $B_{\rm F}$ and $D_{\rm F}$ are not correlated to each other, suggesting that the defects acting as binding sites for BXs are not equivalent to those acting as origins of DE. Based on the distribution of the defects acting as binding sites for BX, an interpretation is given on how the UV peak at RT has a blue shift with the decrease of radius of the nano/microwire.

2. Experiment

ZnO nano/microwires were fabricated by thermal evapouration of pure Zn powder without using a catalyst and were dispersed onto a silicon wafer by skimming it over the as-grown sample ensemble.[8] The sample morphologies were examined by scanning electron microscopy (SEM). Spatially resolved PL measurements were performed using near-field scanning optical microscopy (NSOM) with the excitation at 325 nm from an He–Cd laser via a tapered optical fibre which has a 300-nm aperture. The spatial resolution

†Corresponding author. E-mail: lfeng@sdu.edu.cn

© 2011 Chinese Physical Society and IOP Publishing Ltd

is about 1 μm and the luminescence was detected by a spectrometer with a spectral resolution of 0.8 nm, or ∼ 7 meV at 380 nm. 90 K is a suitable temperature for PL measurement, at which the fine UV peaks can be separated from each other and the defect emissions are detectable.

3. Results and discussion

Three fine UV peaks were separately observed from each nano/microwire at 3.360, 3.308, and 3.235 eV at 90 K. They are mainly assigned to transitions of BX, optical phonon replicas of free excitons FX-1LO and FX-2LO, respectively,[9,10] although each of them may have some minor contributions from other origins. We observed that the BX peak diminished at higher temperatures until the nano/microwire was thermally quenched at about 150 K and that the FX phonon replicas increased all the way, although they could not be resolved above 180 K, which accords well with previous studies[10,11] and justifies the above assignments.

In principle, the density of DFT_{BX} should be proportional to the probability for the FX's to be trapped as BX's. Thus it can be monitored by the fractional intensity of the BX transition in the whole UV emission B_F = (intensity of BX transition)/intensities of all NBE emission peaks at 90 K. The DFT_{Vis} could be determined by the intensity ratio between the DE and the overall emissions, D_F = intensities of DEs/intensities of all NBE emissions and DEs. B_F and D_F can be determined rather accurately thanks to the exclusion of the averaging effect from the sample ensembles.[12]

The changes of B_F and D_F with radius are shown in Figs. 1(a) and 1(b) representatively by two tapered nano/microwires. The two nano/microwires were on the same silicon wafer and should have experienced similar fabrication conditions. As the radius increases, from the position D ($r \sim 100$ nm), to A (150 nm), B (350 nm), E ($\sim$ 500 nm), C ($\sim$ 700 nm), and finally to F ($\sim$ 1 μm) in sequence, B_F decreases all the way from 0.691 to 0.266. More nano/microwires were investigated and confirmed to follow such a trend for B_F. Physically, it appears that the dependence of B_F on size must originate from the changing surface-to-volume ratio, which can be significant for the size on the order of μm or less. A simple model is illustrated in Fig. 2,[13] and the quantitative calculation shows that for ZnO nano/microwires there is a spatially varying distribution of binding site DFT_{BX}'s and the majority condense near the surface. With a large density of DFT_{BX} near the surface, the excitons excited by the 325-nm laser are easier to trap near the defects and exist as BX's. Deeper into the bulk, there are fewer DFT_{BX}'s and the FX's tend to interact with the phonons because ZnO is a highly polar material. Hence for a larger radius, the surface states are less important and the BX transition peak becomes less dominant.

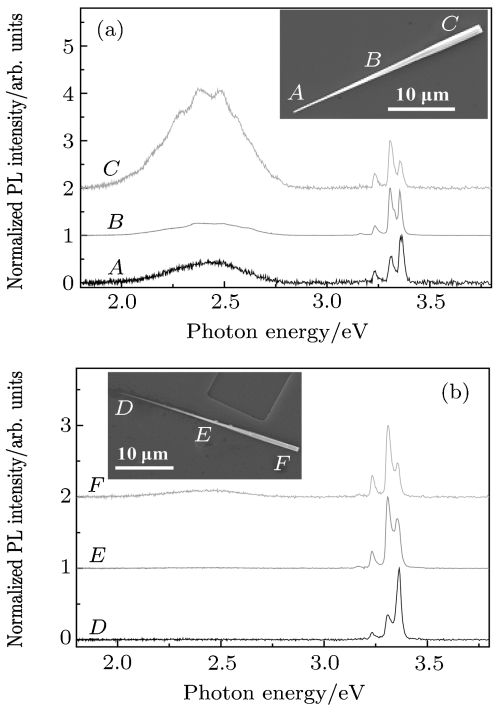


Fig. 1. Spatially resolved PL spectra at 90 K for two tapered ZnO nano/microwires. The insets show the SEM images of the nano/microwires.

In contrast to B_F, D_F does not monotonically change with radius. Comparing positions with similar radii, A and D, E and C, respectively, we may find that the values of B_F are similar but D_F varies a great deal. Therefore, they cannot be the same kind of defect. The UV and visible emissions from ZnO are affected by different kinds of defects. As the radius shrinks, the visible luminescence does not become more dominant, implying that in our samples, DFT_{Vis}'s are distributed in the bulk, not in the surface.[8] The different distributions of the two kinds of defects in our samples make it possible for us to distinguish them through their individual relations to the sizes of the B_F and D_F. For a smaller radius,

B_F is larger, i.e. the 3.360-eV BX transition peak is enhanced and the 3.308-eV FX-1LO and 3.235-eV FX-2LO peaks diminish. Thus the overall energy of the UV peaks increases with shrinking radius. The overall energy of the NBE peaks is only related to the size-dependent DFT_{BX} and is not influenced at all by DEF_{Vis}. So we believe that DEF_{BX} and DEF_{Vis} have no correlation with each other, i.e., the wavelength of the NBE peak is only affected by DEF_{BX} and the visible emissions only originate from DEF_{Vis}'s.

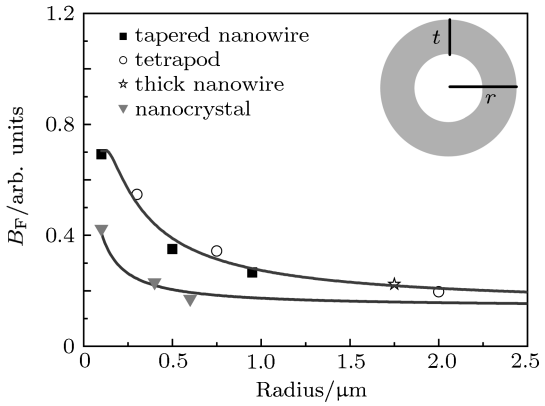


Fig. 2. Experimental (points) and fitted data (solid lines) for B_F for nano/microwires (including tetrapods) and nanocrystals. The inset is a schematic drawing of the cross section of a nano/microwire. The probability of forming BX's is larger in the darker area.

Just like at 90 K, the UV emission also shifts towards a shorter wavelength with the size of ZnO nano/microwire at RT decreasing.[6,14] As shown in Fig. 1, the UV peak blue shift from 3.241 eV (382 nm) to 3.276 eV (378 nm) corresponds to the position shift from F to D at RT.

Below we will discuss how DFT_{BX} induces the blue shift of the NBE peak at RT. The NBE emission is still of excitonic origin at RT. Unlike at 90 K, most of the BX's are released and turn into FX's, because the thermal energy is larger than the localization energy of most BX's ($\sim$ 10 meV) and smaller than the binding energy of FX (60 meV). The FX's are most likely to couple with the phonons in the highly polar ZnO at RT and the NBE peak is mainly composed of FX and FX phonon replicas.[9,15] The relative intensity of the two parts determines the wavelength of the NBE UV peak at RT. The model illustrated in Fig. 2 is still valid here. In the idealized surface layer of the cylinder (whose cross section is a shaded ring belt), the density of DFT_{BX}'s is larger and the thicknesses of the surface layers are assumed to be constant for various radii. It is reasonable to assume the average kinetic energy of FX's to be lower in the surface layer because the FX's may still be attracted slightly by the DFT_{BX} although they are no longer localized. In other words, they are closer to the centre of the Brillouin zone, giving higher efficiency of FX recombination. However, further away from the surface, there is a decreasing number of FX's close to Brillouin zone centre and the simultaneous emissions of photons and LO phonons become a most efficient FX annihilation process.[15] Therefore, at larger radii, with less contribution from the surface layer, the UV peak is at a lower energy position.

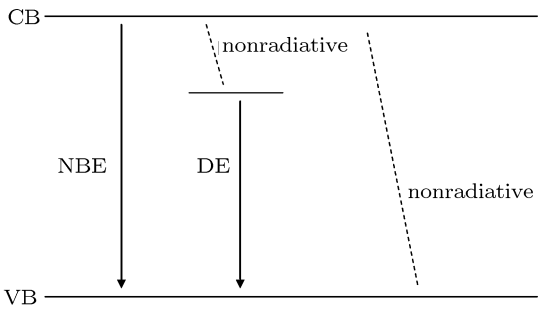


Fig. 3. Radiative and nonradiative processes.

As illustrated in Fig. 3, the two kinds of defects have different energy levels. Electrons are excited into the conduction band. Then (i) they transit nonradiatively into DFT_{Vis} states and recombine with holes generating visible emissions or (ii) they exist as excitons and to the UV peak. Their motion in the material may be influenced by DFT_{BX}'s, e.g. shallow donors, thereby resulting in the wavelength change of the NBE peak. Too many DFT_{Vis}'s may depress the intensity of the UV emission, but exerts no influence on its wavelength.

4. Conclusions

DFT_{Vis} is related to the intensity of visible defect-related emission relative to the UV NBE emission. DFT_{BX} is related to the wavelength of the NBE peak, both at low temperature and at RT. At RT, DFT_{BX} affects the fractions of FX-LO and FX. The two kinds of defects are not correlated to each other. Only DFT_{BX} influences the excitonic origin and then determines the NBE peak position at room temperature.

References

[1] Pearton S J 2003 *J. Appl. Phys.* **93** 1

[2] Cao M S, Li X, Liu Y, Wang F C, Zhai F F and Zhang X X 2007 *Chin. Phys.* **16** 2769

[3] Cox S F J, Davis E A, Cottrell S P, King P J C, Lord J S, Gil J M, Alberto H V, Vilão R C, Duarte J P, Campos N A, Weidinger A, Lichti R L and Irvine S J C 2001 *Phys. Rev. Lett.* **86** 2601

[4] Li S T, Cheng P F, Zhao L and Li J Y 2009 *Acta Phys. Sin.* **58** 523 (in Chinese)

[5] Cui J B 2008 *J. Phys. Chem.* C **112** 10385

[6] Chen C W, Chen K H, Shen C H, Ganuly A, Chen L C, Wu J J, Wen H I and Pong W F 2006 *Appl. Phys. Lett.* **88** 241905

[7] Pan N, Wang X P, Li M, Li F Q and Hou J G 2007 *J. Phys. Chem.* C **111** 17265

[8] Feng L, Cheng C, Lei M, Wang N and Loy M M T 2008 *Nanotechnology* **19** 405702

[9] Hamby D W, Lucca A A, Klopfstein M J and Cantwell G 2003 *J. Appl. Phys.* **93** 3214

[10] Wang L J and Giles N C 2003 *J. Appl. Phys.* **94** 973

[11] Teke A, Özgür Ü, Doğan S, Gu X, Morkoσ H, Nemeth B, Nause J and Everitt H O 2004 *Phys. Rev.* B **70** 195207

[12] Cuong T T, Matthew F and Matthew R P 2008 *Nanotechnology* **19** 415606

[13] Yao B D, Feng L, Cheng C, Loy M M T and Wang N 2010 *Appl. Phys. Lett.* **96** 223105

[14] Yang Y H, Chen X Y, Feng Y and Yang G W 2007 *Nano Lett.* **7** 3879

[15] Shan W, Walukiewicz W, Ager III J W, Yu K M, Yuan H B, Xin H P, Cantwell G and Song J 2005 *Appl. Phys. Lett.* **86** 191911